US Army Corps of Engineers®

Leaky Internal-Barrier Normal-Flow Boundaries in the ADCIRC Coastal Hydrodynamics Code

by J. J. Westerink, R. A. Luettich, and A. Militello

PURPOSE: This Coastal and Hydraulic Engineering Technical Note (CHETN) describes the methodology and input requirements for the leaky-barrier boundary feature in the Advanced Circulation (ADCIRC) coastal hydrodynamics code versions 40.02 and higher. This feature calculates flow over and through structures such as levees and jetties.

BACKGROUND: The ADCIRC hydrodynamic model has been developed for the U.S. Army and Navy over the past 12 years to compute long wave circulation in coastal oceans associated with tides, winds, and density-driven flow (Luettich, Westerink, and Scheffner 1991; Westerink et al. 1992b). ADCIRC is based on a reformulation of the shallow water equations and applies a finite element discretization strategy. The specific strategies applied give accurate numerical solutions free from artificial noise or spurious oscillations. Therefore ADCIRC does not require the addition of artificially high viscosity in order to obtain smooth and stable solutions. The model permits application of highly unstructured grids with great detail specified locally. ADCIRC's basic formulation and algorithms have been extensively verified through analysis of the algorithms and comparison to analytical solutions (Kolar et al. 1994 a,b; Kolar, Gray, and Westerink 1996; Luettich, Westerink, and Scheffner 1991; Luettich et al. 1992; Luettich, Hu, and Westerick 1994; Luettich and Westerink 1991; Westerink et al. 1994).

ADCIRC has been validated in tidal- and wind-driven ocean, shelf and estuarine applications around the world (Blain et al. 1993; Blain, Westerink, and Luettich 1994, 1998; Grenier, Luettich, and Westerink 1994, 1995; Hagen, Westerink, and Kolar 2000; Hagen et al. 2001; Hench et al. 1994; Luettich, Birkhahn, and Westerink 1991; Luettich and Westerink 1995a; Scheffner et al. 1994; Westerink and Luettich 1991, 1997; Westerink, Muccino, and Luettich 1992; Westerink et al. 1992a; Westerink, Luettich, and Scheffner 1993; Westerink, Luettich, and Muccino 1994; Westerink 1993). Recently ADCIRC has incorporated flood wave propagation over initially dry land, flood wave recession from initially wet regions, and barriers such as levees or jetties that are treated as weirs (Luettich and Westerink 1995b,c, 1999; Westerink and Luettich 1996). This CHETN describes the modification of ADCIRC to include leaky or permeable barriers.

ADCIRC Versions 40.02 and higher include modifications that allow internal-barrier boundaries, which lie entirely within the domain, to be specified as leaky barriers to represent large holes that connect both sides of the barrier. This leaky internal-barrier boundary feature has been implemented by adding cross-barrier pipes to the existing internal-barrier boundaries. Thus, ADCIRC now allows the user to specify two basic types of internal boundary barriers. One type is the existing internal-barrier flow boundaries that act as weirs that can be overtopped. This representation describes a levee or jetty that is being overtopped. The second type is the new leaky internal-barrier flow boundaries that allow cross-barrier flow once the crown of the pipe

placed within the barrier is submerged at one or both ends. This representation describes a levee or jetty with large holes or drainage pipes through which flow can pass from one side to the other. Flow can also pass over the top of these levees or jetties once the water surface overtops the crest. Thus, the cross-barrier pipe flow can occur in combination with any cross-barrier flow that overtops the barrier. This CHETN describes the basic methodologies implemented, the input changes in the ADCIRC code, and two example cases.

METHODOLOGY FOR LEAKY INTERNAL-BARRIER BOUNDARIES: The best way to accommodate large holes and openings in barriers, which permit a significant amount of cross-barrier flow, is to add cross-barrier pipes to the existing internal-barrier boundaries based on weirs. Modifications have been made in ADCIRC Version 40.02 and higher to allow the specification of leaky internal-barrier boundaries that transmit flow through the barrier using pipe formulae and over the top of the barrier using weir formulae. The new leaky-internal barrier boundary is an addition to all the boundary condition types that were in place in earlier versions of ADCIRC. All other boundary types are specified and handled as in previous versions of ADCIRC. Six cross-barrier pipe configurations have been included and are described.

Configuration 1: Water Level on Both Sides of the Internal Barrier Below the Height of the Crown of the Cross-Barrier Pipe

Water on both sides of the internal barrier is below the height of the crown of the cross-barrier pipe (Figure 1). Thus

$$\zeta_L < h_p \text{ and } \zeta_R < h_p \tag{1}$$

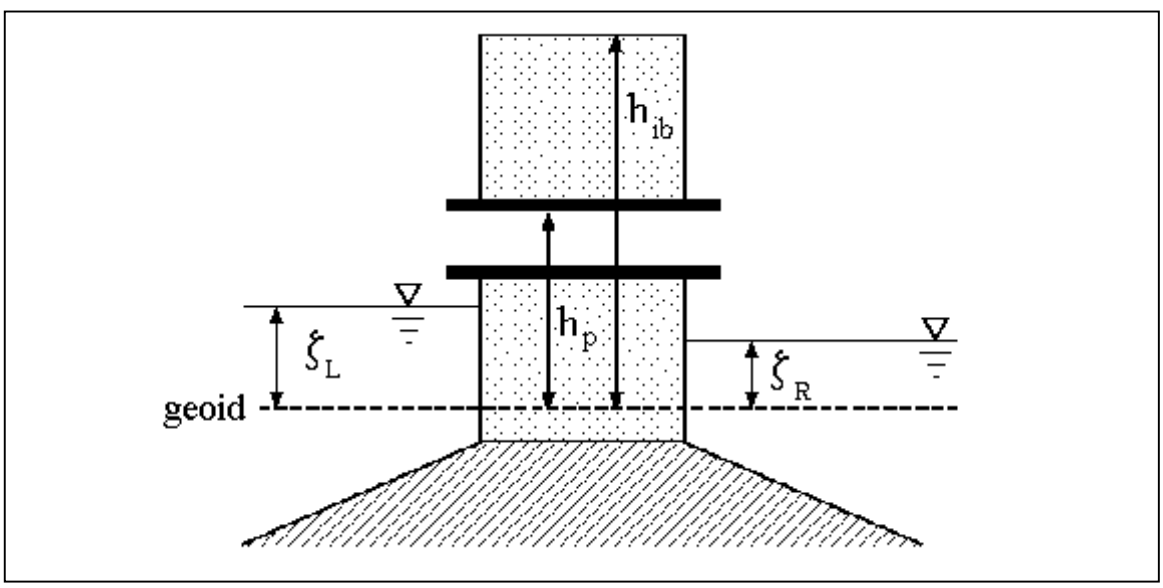

Figure 1. Water level on both sides of the barrier below the height of the crown of the cross-barrier pipe

where

ζ_L = water elevation on the front side of the internal barrier relative to the geoid (the hypothetical surface around the Earth that is everywhere normal to the direction of gravity and coincides with mean sea level in the oceans),

ζ_R = water elevation on the back side of the internal barrier relative to the geoid and

h_p = elevation of the crown of the cross barrier pipe relative to the geoid.

There is no cross-barrier flow through the pipe. Thus, the cross-barrier flow equals:

$$Q_n = 0 \tag{2}$$

It is assumed that flow through the cross-barrier pipe is negligible if both sides of the pipe are only partially submerged. This assumption is reasonable when comparing the amount of through flow when at least one end of the pipe is fully submerged.

Configuration 2: Water Level on Both Sides of the Internal Barrier Equal

Water elevation is equal on both sides of the internal barrier (Figure 2). Thus

$$\zeta_L = \zeta_R \tag{3}$$

There is no cross-barrier flow through the pipe. Thus, the cross-barrier flow equals:

$$Q_n = 0 \tag{4}$$

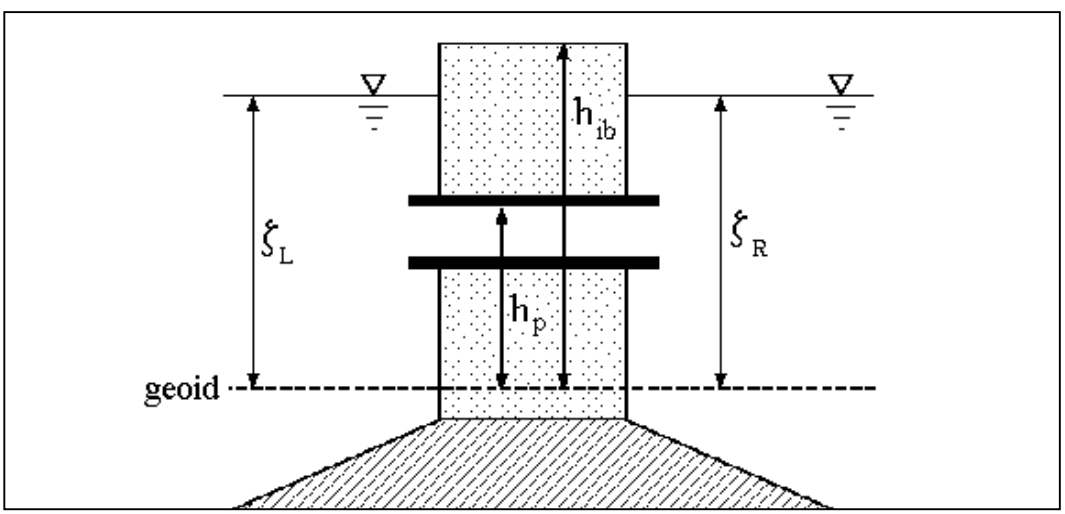

Figure 2. Water level on both sides of the internal barrier equal

Configuration 3: Water Elevation on the Front Side of the Internal Barrier Greater than Water Elevation on the Back Side; Water Elevation on the Front Side Greater than the Crown Height of the Cross-Barrier Pipe; and Water Elevation on the Back Side Below Crown Height of the Pipe

Water elevation on the front side of the internal barrier is greater than water elevation on the back side, water elevation on the front side is greater than the crown height of the cross-barrier pipe and water elevation on the back side is below the crown height of the pipe (Figure 3). Thus

$$\zeta_L > \zeta_R \tag{5}$$

$$\zeta_L \geq h_p \text{ and } \quad \zeta_R < h_p \tag{6}$$

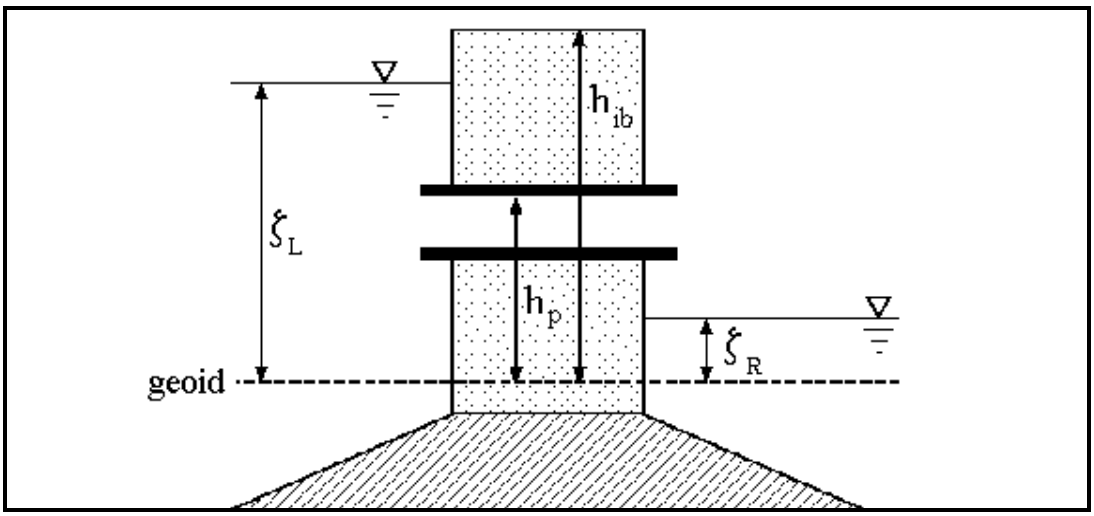

Figure 3. Water elevation on the front side of the internal barrier greater than water elevation on the back side; water elevation on the front side greater than the crown height of the cross-barrier pipe; and water elevation on the back side below crown height of the pipe

Cross-barrier flow through the pipe is from the front face to the back face. Flow can be computed by applying the Bernoulli equation to the pipe section crossing the internal barrier. This situation results in a free discharging flow through the pipe from front to back computed as (Daugherty et al. 1985):

$$Q_n = \frac{\pi D^2}{4}\sqrt{\frac{2g(\zeta_L - h_p)}{1+\frac{fL}{D}}} \tag{7}$$

where

$D =$ cross-barrier pipe diameter

$g =$ gravity

$\frac{fL}{D}$ = the bulk pipe friction factor for the cross-barrier pipe

f = classical pipe friction coefficient

L = length of pipe through the barrier.

It is assumed that if the back face opening of the pipe is partially submerged, and the discharge can be approximated as a free discharge. The classical pipe friction factor f is dependent on Reynolds number for the pipe, $R = \frac{DV}{\nu}$ where ν = kinematic viscosity of water as well as the relative roughness of the pipe. The pipe friction factor ranges between 0.0001 to 0.1 and diagrams with values are presented in any standard fluid mechanics text (e.g., Daugherty et al. 1985). It is also noted that the length of the pipe through the barrier typically equals the width of the barrier unless the opening through the barrier is tortuous in which case it should be increased.

Configuration 4: Water Elevation on the Front Side of the Internal Barrier Greater than Water Elevation on the Back Side; Water Elevation on the Front Side Greater than the Crown Height of the Cross Barrier Pipe; and Water Elevation on the Back Side Above the Crown Height of the Pipe

Water elevation on the front side of the internal barrier is greater than water elevation on the back side; water elevation on the front side is greater than the crown height of the cross-barrier pipe; and water elevation on the back side is above the crown height of the pipe (Figure 4). Thus

$$\zeta_L > \zeta_R \tag{8}$$

$$\zeta_L \geq h_p \text{ and } \quad \zeta_R \geq h_p \tag{9}$$

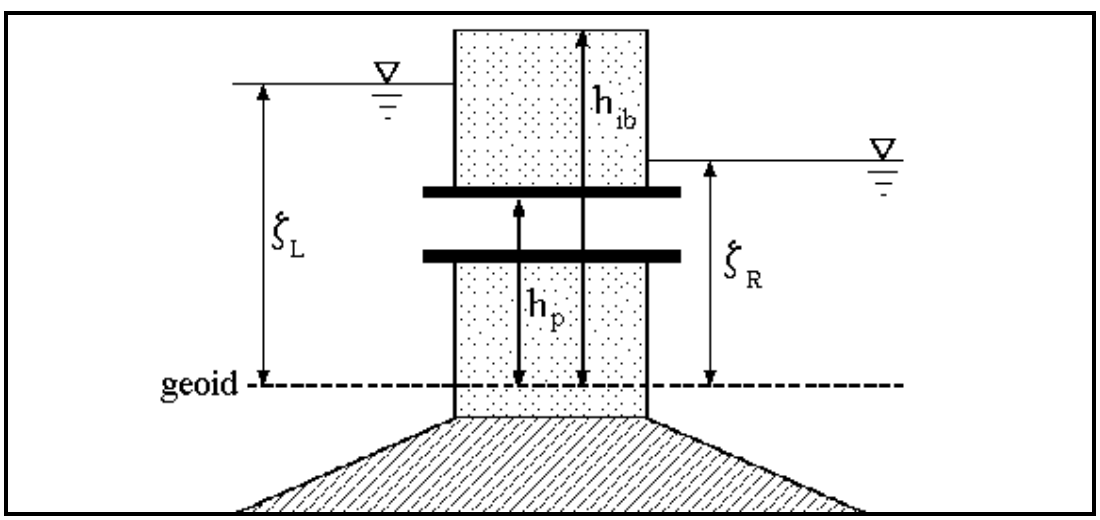

Figure 4. Water elevation on the front side of the internal barrier greater than water elevation on the back side; water elevation on the front side greater than the crown height of the cross-barrier pipe; and water elevation on the back side above crown height of the pipe

Cross-barrier flow through the pipe is from the front face to the back face. Flow can be computed by applying the Bernoulli equation to the pipe section crossing the internal barrier. This calculation results in a submerged discharging flow through the pipe from front to back computed as:

$$Q_n = \frac{\pi D^2}{4}\sqrt{\frac{2g(\zeta_L - \zeta_R)}{\frac{fL}{D}}} \tag{10}$$

Configuration 5: Water Elevation on the Back Side of the Internal Barrier Greater than Water Elevation on the Front Side; Water Elevation on the Back Side Greater than the Crown Height of the Cross-Barrier Pipe; and Water Elevation on the Front Side Below the Crown Height of the Pipe

Water elevation on the back side of the internal barrier is greater than water elevation on the front side; water elevation on the back side is greater than the crown height of the cross-barrier pipe; and water elevation on the front side is below the crown height of the pipe (Figure 5). Thus

$$\zeta_R > \zeta_L \tag{11}$$

$$\zeta_R \geq h_p \text{ and } \zeta_L < h_p \tag{12}$$

Cross-barrier flow through the pipe is from the back face to the front face. Flow can be computed by applying the Bernoulli equation to the pipe section crossing the internal barrier.

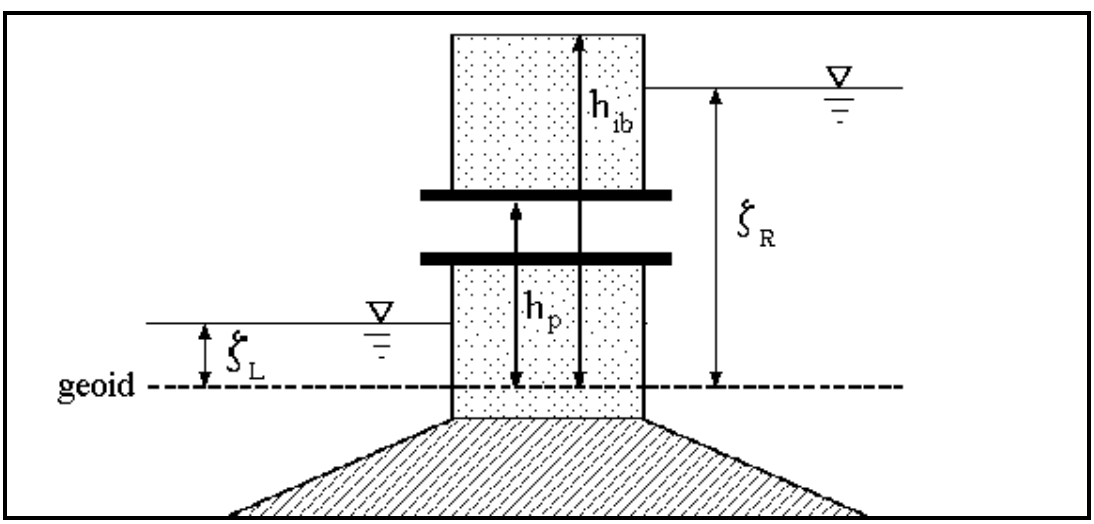

Figure 5. Water elevation on the back side of the internal barrier greater than water elevation on the front side; water elevation on the back side greater than the crown height of the cross-barrier pipe; and water elevation on the front side below crown height of the pipe

This calculation results in a free discharging flow through the pipe from back to front computed as:

$$Q_n = \frac{\pi D^2}{4}\sqrt{\frac{2g(\zeta_R - h_p)}{1+\frac{fL}{D}}} \tag{13}$$

It is assumed that if the front face opening of the pipe is partially submerged, the discharge can be approximated as a free discharge.

Configuration 6: Water Elevation on the Back side of the Internal Barrier Greater than Water Elevation on the Front Side; Water Elevation on the Back Side Greater than the Crown Height of the Cross-Barrier Pipe; and Water Elevation on the Front Side Above the Crown Height of the Pipe

Water elevation on the back side of the internal barrier is greater than water elevation on the front side; water elevation on the back side is greater than the crown height of the cross-barrier pipe; and water elevation on the front side is above the crown height of the pipe (Figure 6). Thus

$$\zeta_R > \zeta_L \tag{14}$$

$$\zeta_R \geq h_p \text{ and } \zeta_L \geq h_p \tag{15}$$

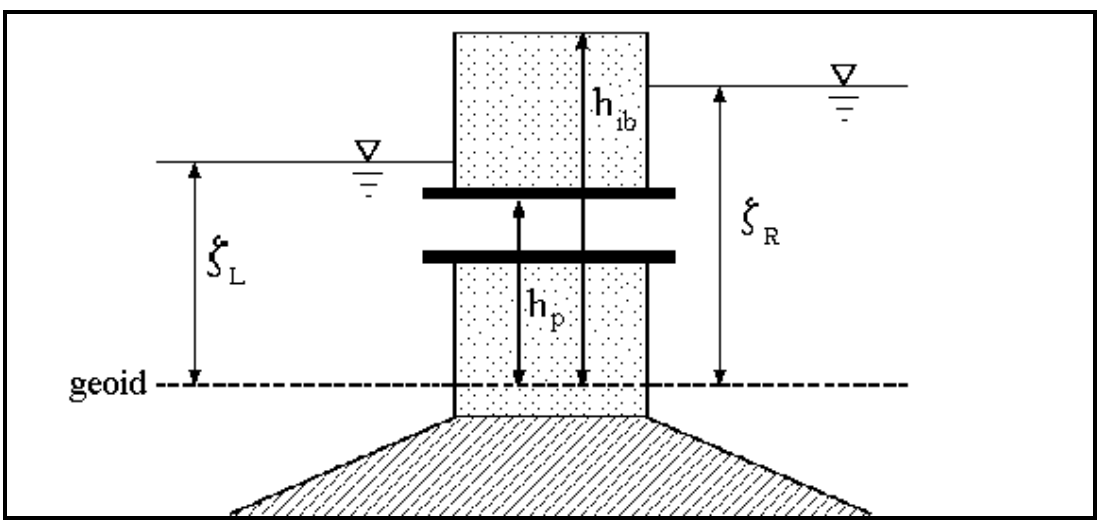

Figure 6. Water elevation on the back side of the internal barrier greater than water elevation on the front side; water elevation on the back side greater than the crown height of the cross-barrier pipe; and water elevation on the front side above crown height of the pipe

Cross-barrier flow through the pipe is from the back face to the front face. Flow can be computed by applying the Bernoulli equation to the pipe section crossing the internal barrier. This calculation results in a submerged discharging flow through the pipe from back to front computed as:

$$Q_n = \frac{\pi D^2}{4}\sqrt{\frac{2g(\zeta_R - \zeta_L)}{\frac{fL}{D}}} \tag{16}$$

The leaky internal-barrier boundaries retain the same overtopping ability as the standard internal-barrier boundaries in earlier versions of ADCIRC. The basic assumption for overtopping is that when surface-water elevation exceeds the height of the internal barrier, h_{ib}, the internal-barrier boundary section overtops. In this case, weir formulae (Chow 1959) are applied to compute free-surface subcritical or supercritical inflow/outflow across the internal-barrier boundary, which is added to the cross-barrier pipe flows. The computed normal cross-barrier flows have been implemented within the framework of normal-flow boundary conditions and it is possible to specify either one of the following two implementations.

Implementation 1: Essential Leaky Internal-Barrier Normal-Flow Boundary with Free Tangential Slip Allowed

The portion of the boundary integral in the Generalized Wave-Continuity Equation (GWCE) (Luettich, Westerink, and Scheffner 1991) corresponding to the leaky internal-barrier boundaries is evaluated using the calculated nodal cross-barrier flux values. Nodal values of flux are computed as defined in configurations 1 through 6. Nodal flux is assumed to vary linearly between nodes on each internal-barrier boundary segment when the flow integral in the GWCE is computed. Furthermore, the normal-direction velocity component is computed by dividing the flux by the total water column at the node of interest. This value of normal velocity is enforced in the momentum equations by eliminating the normal-direction momentum equation at the internal-barrier boundary nodes (obtained after reorienting the *x-y* momentum equations into *n-t* directions) and replacing this equation with the nodal velocity value. The tangential-direction momentum equation at internal-barrier boundary nodes is not modified allowing for free tangential slip. This procedure does result in model-predicted normal flows (computed with the predicted nodal velocities and elevations) on leaky internal-barrier boundaries exactly matching the value as computed by summing the Bernoulli-based pipe flow added to the broad-crested weir formula flow.

Enforcing essential normal-flow boundary conditions on internal barriers can overconstrain the system and set up local oscillatory modes. This situation has been observed in a variety of application cases. In practical applications, leaky internal-barrier boundary conditions are typically implemented as natural conditions as described in the following paragraph.

Implementation 2: Natural Leaky Internal-Barrier Normal-Flow Boundary with Free Tangential Slip Allowed

The portion of the boundary integral in the GWCE corresponding to the leaky internal-barrier boundaries is evaluated using the calculated nodal cross-barrier flux values. Nodal values of flux are computed as defined in configurations 1 through 6. Nodal flux is assumed to vary linearly between nodes on each internal-barrier boundary segment when the flow integral in the GWCE is computed. Neither the normal- or tangential-direction momentum equations at internal-barrier

boundary nodes are modified. Therefore, normal flows on internal-barrier boundaries exactly match the value computed by summing the Bernoulli-based pipe flow added to the broad-crested weir formula flow in the limit as grid size becomes small. The procedure allows for free tangential slip.

MODIFIED INPUT REQUIREMENTS FOR ADCIRC VERSION 40.02 AND HIGHER: In order to specify a leaky internal-barrier boundary, the following boundary information must be specified in the unit 14 (grid) input file.

Leaky internal-barrier flow boundary segments are input as normal flow (or discharge) boundary segments with boundary type, ***IBTYPE***, designated equal to either 5 or 25 depending on the exact treatment desired for the leaky internal-barrier boundaries. Each leaky internal boundary is input as a normal-flow boundary segment. The following information is provided for each leaky internal-barrier boundary segment:

NVELL(K), IBTYPE: For each leaky internal-barrier boundary segment; these values are directly followed by the boundary-node pairs within the segment and other information for the leaky-barrier boundary-node pairs.

NVELL(K) = The number of leaky internal-boundary node pairs on a particular segment.

IBTYPE = 5: Essential leaky internal-barrier normal-flow boundary with free tangential slip allowed. The leaky internal (island type) barrier boundary allows free surface subcritical and supercritical normal cross-barrier inflow and outflow once the barrier has been overtopped. Cross-barrier pipes are located under the top of the barrier which allow free discharging, full-pipe cross-barrier inflow/outflow and submerged discharging, full-pipe cross-barrier inflow/outflow once water level rises above the crown of the pipe on at least one side of the barrier. The computed cross-barrier flow is treated as an essential boundary condition. Tangential slip is allowed. This boundary condition applies to weir-type barriers that have cross-barrier pipes. The barrier lies entirely within the computational domain. Normal-flow computations for the weir and pipe component flows are based on water elevations on both sides of the barrier.

IBTYPE = 25: Natural leaky internal-barrier normal-flow boundary with free tangential slip allowed. The leaky internal (island type) barrier boundary allows free surface subcritical and supercritical normal cross-barrier inflow and outflow once the barrier has been overtopped. Cross-barrier pipes are located under the top of the barrier that allow free discharging, full-pipe cross-barrier inflow/outflow and submerged discharging, full-pipe cross-barrier inflow/outflow once water level rises above the crown of the pipe on at least one side of the barrier. The computed cross-barrier flow is treated as a natural boundary condition. Tangential slip is allowed. This boundary condition applies to weir-type barriers that have cross-

barrier pipes. The barrier lies entirely within the computational domain. Normal-flow computations for both the weir and pipe component flows are based on water elevations on both sides of the barrier.

If any leaky internal-barrier normal-flow boundaries are designated in the unit 14 input file (***IBTYPE*** = 5 and/or 25), the following information is required for each leaky barrier node pair that defines the leaky internal-barrier boundary segment.

NBVV(K,I), IBCONN(I), BARINHT(I), BARINCFSB(I), BARINCFSP(I), PIPEHT(I), PIPECOEF(I), PIPEDIAM(I) for the ***I=1,NVELL(K***) node pairs in the leaky internal-barrier boundary segment ***K.***

NBVV(K,I) = front-face node for the leaky internal-barrier boundary

IBCONN(I) = the paired back-face node for the leaky internal-barrier boundary

BARINHT(I) = h_{ib} = the height of the leaky internal barrier above the geoid (positive above the geoid and negative below the geoid),

BARINCFSP(I) = the coefficient of supercritical free surface flow (typical value = 1.0) at the leaky internal-barrier boundary node pair. This coefficient is applied if the cross-barrier flow is supercritical.

BARINCFSB(I) = the coefficient of subcritical free-surface flow (typical value = 1.0) at the leaky internal-barrier boundary node pair. This coefficient is applied if the cross-barrier flow is subcritical.

PIPEHT(I) = h_p = cross-barrier pipe crown elevation above the geoid (positive above the geoid and negative below the geoid) at the specific boundary node pair. ***PIPEHT(I)*** must exceed the input bathymetric values specified at the associated global node and at the paired node. Accounting for sign conventions for bathymetry and cross-barrier pipe crown height, we must satisfy the conditions:

PIPEHT(I).GE.-DP(NBVV(K,I)) and
PIPEHT(I).GE.-DP(IBCONN(I)).

If these conditions are not satisfied, the code will stop.

PIPECOEF(I) = the bulk pipe friction factor for the specified leaky internal-barrier with cross-barrier pipe boundary node pair. This bulk friction factor is defined as:

$$\boldsymbol{PIPECOEF} = \frac{fL}{D}$$

where

f = Classical pipe friction coefficient
L = Length of pipe through the barrier (in consistent units).
D = Diameter of the cross-barrier pipe (in consistent units).

PIPEDIAM(I) = *D* = Diameter of the cross-barrier pipe (in consistent units).

This defined format is similar to that of the standard ***IBTYPE***= 4, 24 internal-barrier boundary except that values for ***PIPEHT(I)***, ***PIPECOEF(I)*** and ***PIPEDIAM(I)*** must be specified. Furthermore, as is the case with the standard internal-barrier boundary, the leaky internal-barrier must be defined as an island with parallel front and back faces so that there is a one-to-one correspondence between the nodes on the front face of the internal-barrier boundary and the nodes on the back face. This correspondence is to allow the comparison of water levels on both sides of the barrier, which is the basis of the cross-barrier flow computations. Only node numbers on the front side of the barrier are provided as input for the array ***NBVV(K,I)***. Thus global node numbers describing the front of the internal barrier are input sequentially and defined as ***NBVV(K,I)***, where ***K*** = flow boundary segment and ***I*** = sequential flow boundary node, for the front side of the internal-barrier boundary in a clockwise direction (this convention has been standard for all internal boundaries) while the paired backside global node numbers are specified in ***IBCONN(I)***. All other information, ***BARINHT(I)***, ***BARINCFSP(I)***, ***BARINCFSB(I), PIPEDIAM(I), PIPECOEF(I)*** and ***PIPEDIAM(I)*** are provided along with ***NBVV(K,I)*** and ***IBCONN(I)*** for each front side node.

No changes are required in the unit 15 (control) input file to accommodate the leaky internal-barrier boundary condition. All specified normal-flow external boundary and external/internal-barrier normal-flow boundary information is output to the unit 16 output file with additional detailed boundary segment information. Normal flows at either specified normal-flow external boundary nodes or external/internal-barrier boundary nodes can be tracked using the specified unit 61 and 62 station output file features with appropriately specified coordinates.

All input and output requirements and/or changes are thoroughly described in the html-based on-line documentation file for ADCIRC Version 40.02 and higher. The Web site is *http://www.unc.edu/depts/marine/C_CATS/adcirc/* and contains a full description of the model as well as the input files described in the following examples.

Idealized Example 20c: Example 20c is a modified version of our standard test case for verifying overtopping levees, which now includes the new feature, leaky barriers. The input files for this case are the unit 14 and 15 files designated *example20c.grd* and *example20c.inp*, respectively. These files can be obtained at *http://www.unc.edu/depts/marine/C_CATS/adcirc/*. This case incorporates three internal-barrier boundaries that are shown in Figure 7. The first is designated in the unit 14 input file as flow boundary no. 8 and encircles the southern low-lying land region. This barrier has been set up to allow for both overtopping as well as leakage through the barrier itself. The crown of this internal barrier occurs 0.6096 m (2.0 ft) above the geoid. In addition to barrier overtopping, this barrier incorporates the leaky internal-barrier boundary to account for the possibility of holes that can lead to cross-barrier flow. The leaky internal-barrier boundary option is implemented with cross-barrier pipes that are located under the crown of the barrier. This boundary must either be designated as ***IBTYPE*** = 5 or 25. In this case we have designated ***IBTYPE*** = 25 so that the computed cross-barrier flow will be implemented as a natural boundary condition. This specification generally avoids over-constraining the system of equations and reduces the possibility of cross-barrier spurious modes. In addition to the standard internal-barrier information, the user must designate the height of the

crown of the cross-barrier pipe, a friction factor for the cross-barrier pipe, and the diameter of the cross-barrier pipe for each of the internal barrier with cross-barrier pipe boundary-node pairs.

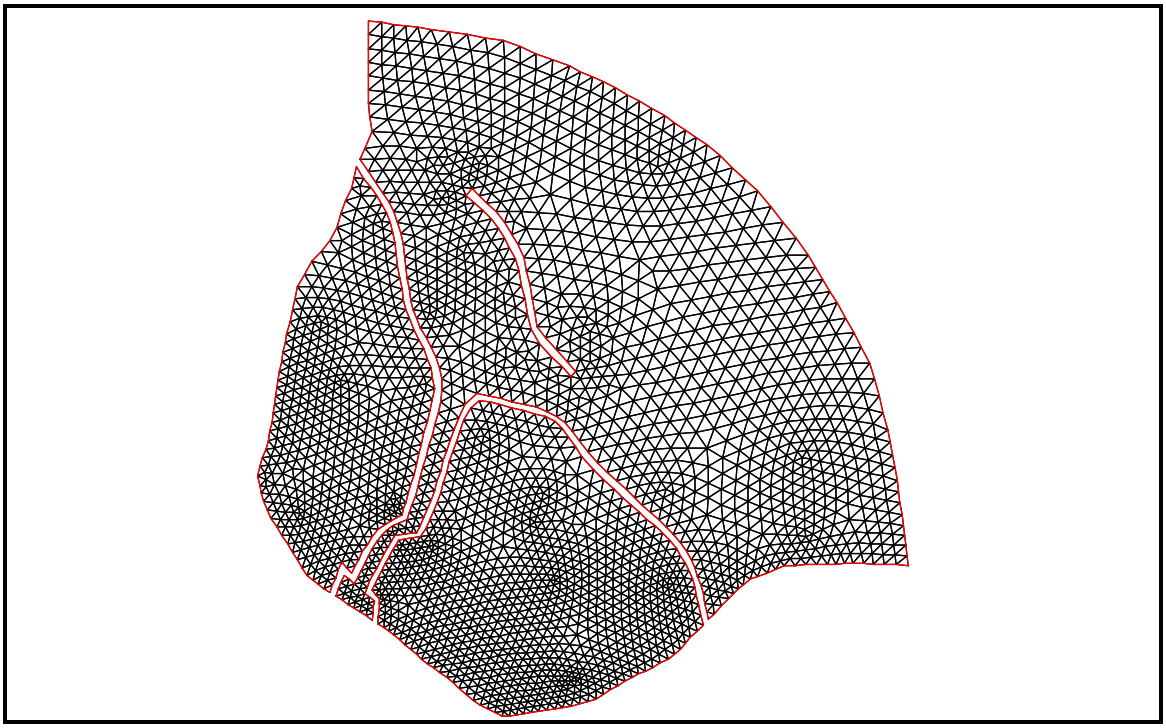

Figure 7. Domain definition and finite element grid for Example 20c

Flow boundary no. 8 has been implemented as a leaky boundary by specifying four node pairs as having a pipe crown height located at ***PIPEHT*** = 0.3048 m (1.0 ft), a pipe friction factor ***PIPECOEF*** = 0.1, and a pipe diameter ***PIPEDIAM*** = 0.6096 (2.0 ft). At all boundary node pairs where no cross-barrier pipe flow is desired, a pipe crown height equal to 30.48 m (100 ft) has been specified. Note that leakage is only initiated once the water level exceeds designated pipe crown height, ***PIPEHT***. The second barrier is designated in the unit 14 input file as flow boundary no. 9 and encircles the western low-lying land region and has an internal-barrier boundary height of 0.762 m (2.5 ft). Finally, the third is designated in the unit 14 input file as flow boundary no. 10 and lies northeast of the river and has an internal-barrier boundary height of 0.3048 m (1.0 ft). The finite-element grid and the bathymetry are shown in Figures 7 and 8, respectively.

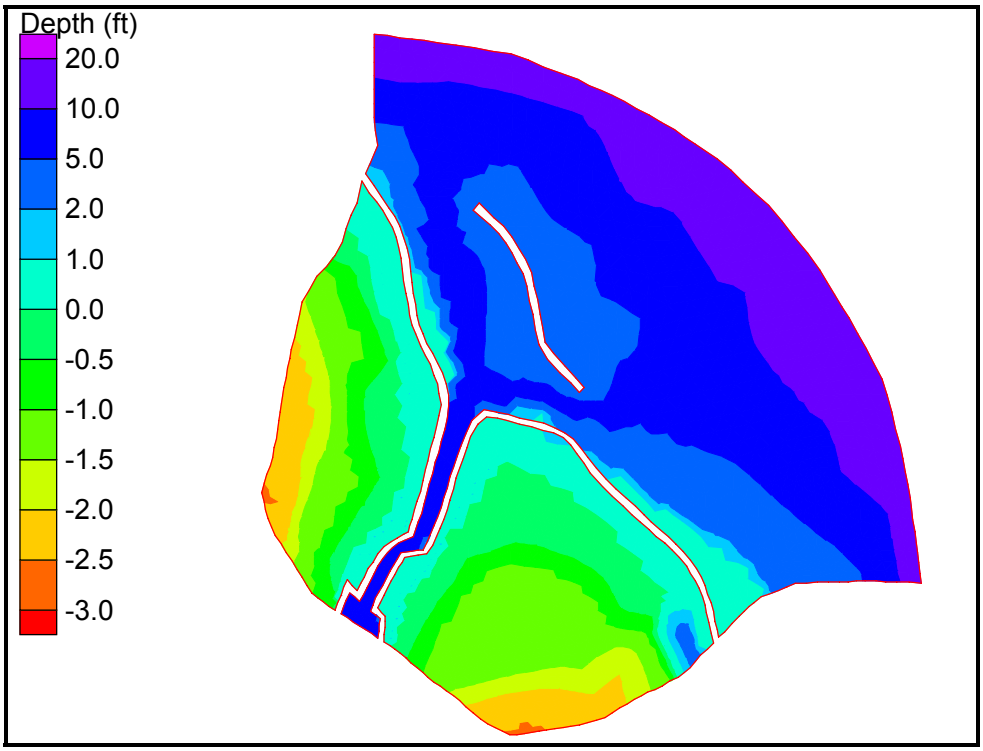

Figure 8. Definition of bathymetry in feet with respect to the geoid for Example 20c

The simulation is forced with an open-ocean surface-elevation forcing equal to 1.524 m (5.0 ft) at a frequency of 0.25 cycles/day so that the water reaches its maximum level after 1 day of simulation. This case was run with ADCIRC release 41.05. Results are shown in Figures 9 through 12. Figure 9 shows the leaky barrier starting to transmit water through the northern side of the internal-barrier boundary, which encompasses the southern low-lying land once water elevation exceeds 0.3048 m (1.0 ft) in front of the levee. When the water level in front of this barrier exceeds 0.6096 m (2 ft), cross-barrier overtopping occurs as well (Figure 10). Eventually water level rises in excess of 1.2192 m (4.0 ft). Water then starts to recede from the southern low-lying land through both the cross-barrier pipes and over the top of the barrier (Figure 11). Once the water level within the southern low-lying land drops below 0.6096 m (2 ft), drainage from the low-lying land over the top of the barrier stops and drainage is strictly through the pipes that have been placed in the barrier (Figure 12). This drainage will continue until the water level in the southern low-lying land is equal to 0.3048 (1.0 ft).

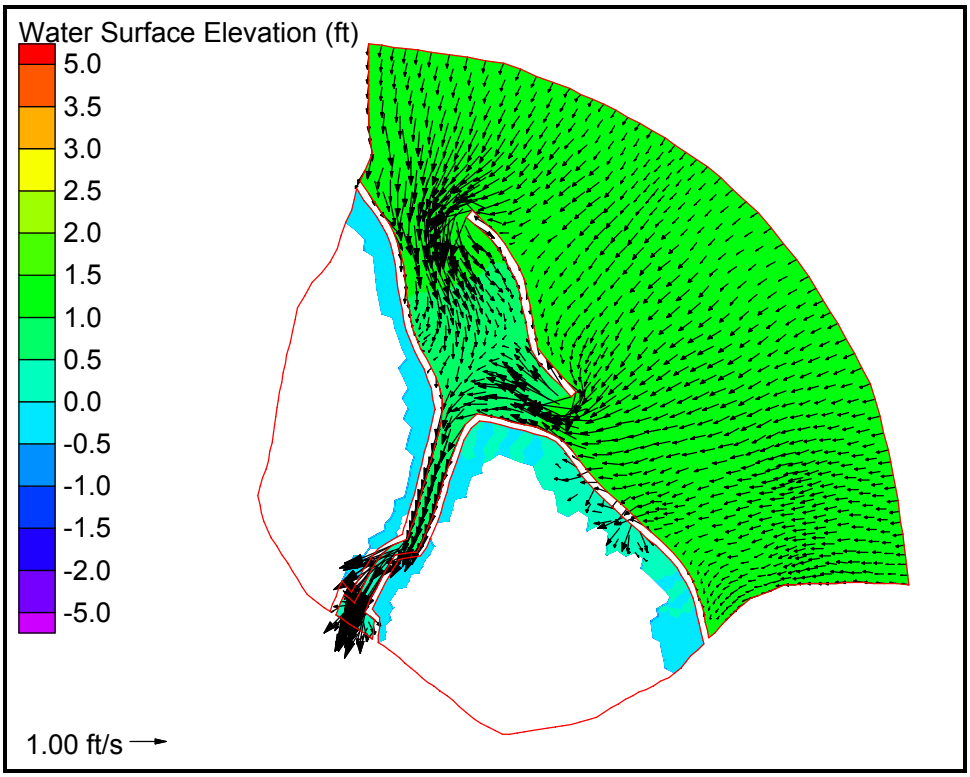

Figure 9. Example 20c elevation and velocity solution at 0.06 days

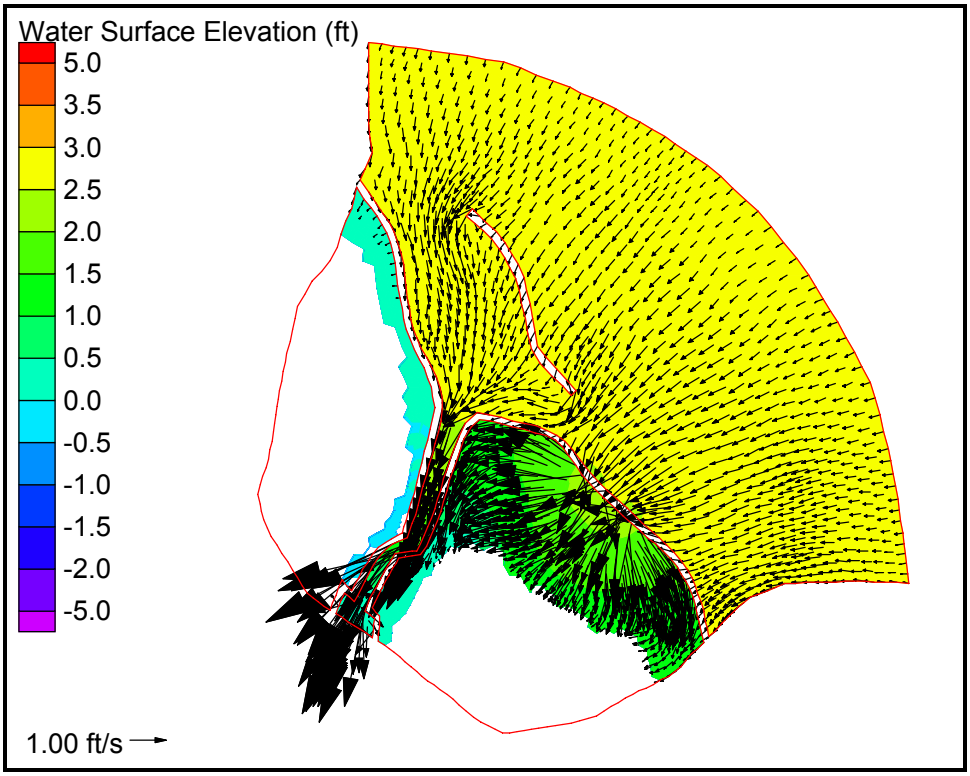

Figure 10. Example 20c elevation and velocity solution at 0.16 days

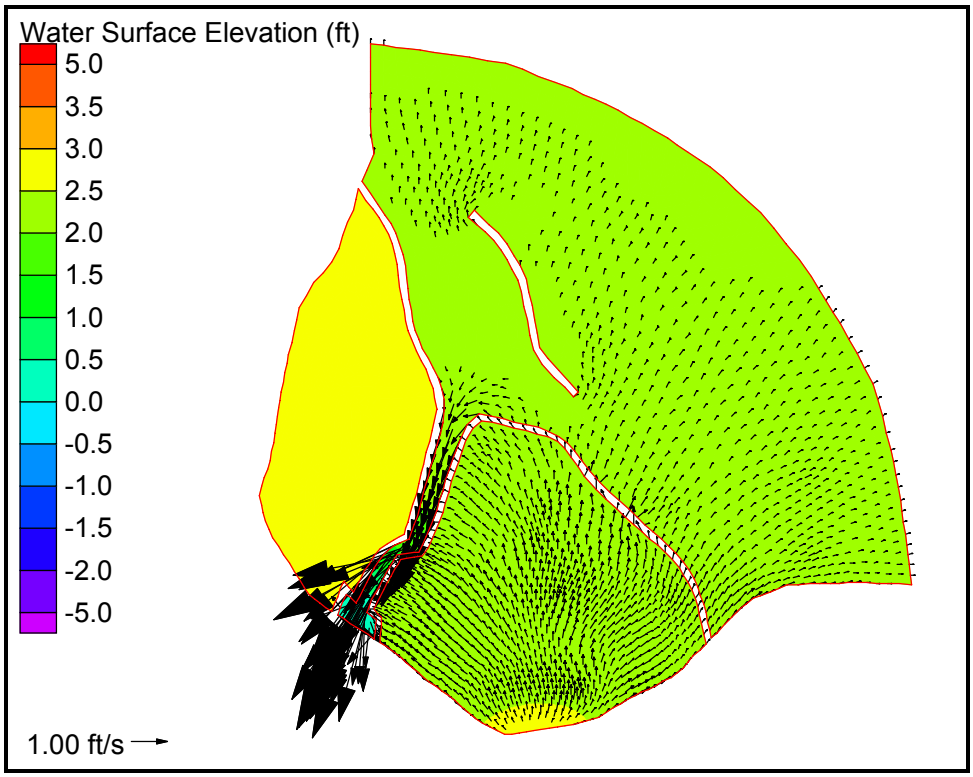

Figure 11. Example 20c elevation and velocity solution at 0.70 days

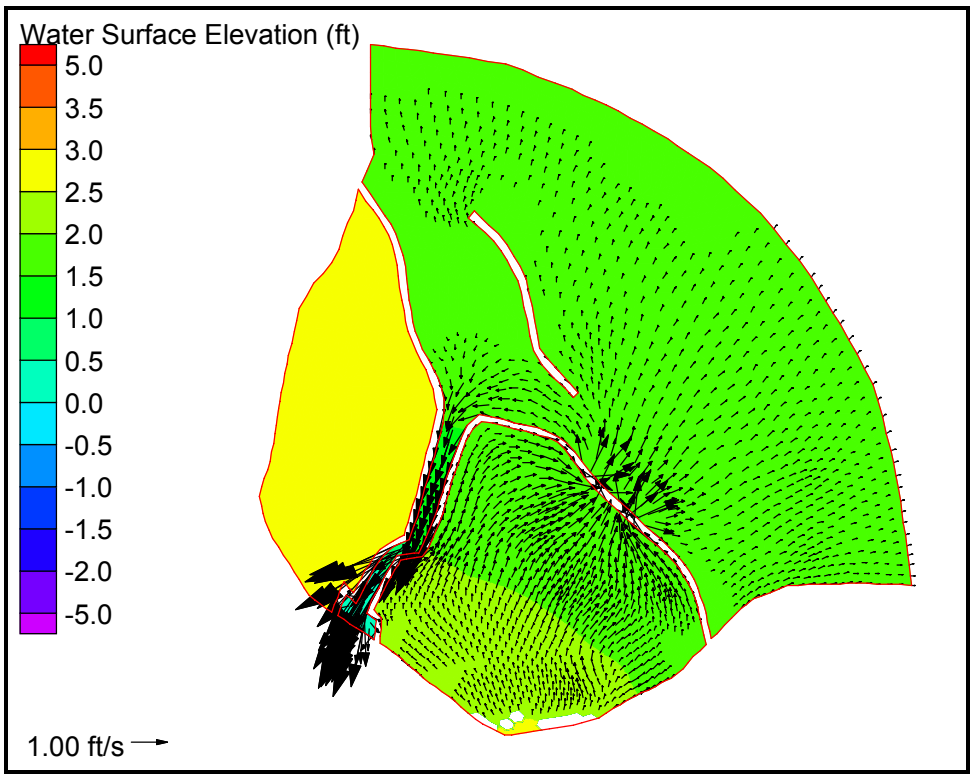

Figure 12. Example 20c elevation and velocity solution at 0.80 days

Example Applied to Grays Harbor, Washington: The Grays Harbor sample problem represents an intermediate-sized domain situated in the Pacific Ocean off of the State of Washington and the province of British Columbia. The domain and finite element grid are shown in Figure 13 and bathymetry/topography are shown in Figure 15. Grays Harbor is highly resolved in the domain and Willapa Bay is represented with medium resolution. Lower-resolution representations of the Columbia Estuary, the Strait of Juan de Fuca, the Strait of Georgia and Queen Charlotte Sound are included.

The input files are *grays_s03_g04_r11.grd* (unit 14) and *grays_s03_g04_r11.inp* (unit 15) which are available on the Web at *http://www.unc.edu/depts/marine/C_CATS/adcirc/*. The partially-submerged jetty to the south of the inlet at Grays Harbor is represented as an internal-barrier boundary (Figures 14 and 16). This barrier has been set up to allow for both overtopping and leakage through the barrier itself. The crown of this internal barrier ranges between 1.5 m below the geoid along the western portion of the jetty to 3.0 m above the geoid along its eastern portion. In addition to barrier overtopping, this barrier incorporates the leaky internal-barrier boundary to account for the possibility of holes in barriers that can lead to cross-barrier through flow. Two nodes have been set up to allow leaky through flow in the region where the jetty rises above the geoid. This boundary has been designated as ***IBTYPE*** = 25 so that the computed cross-barrier through and over flow will be implemented as a natural boundary condition. This flow boundary has been implemented as a leaky boundary by specifying two node pairs as having a pipe crown height located at ***PIPEHT*** = 1.0 m, a pipe friction factor ***PIPECOEF*** = 0.1, and a pipe diameter ***PIPEDIAM*** = 0.25 m. At all boundary node pairs where no cross-barrier pipe flow is desired, a pipe crown height equal to 100 m has been specified.

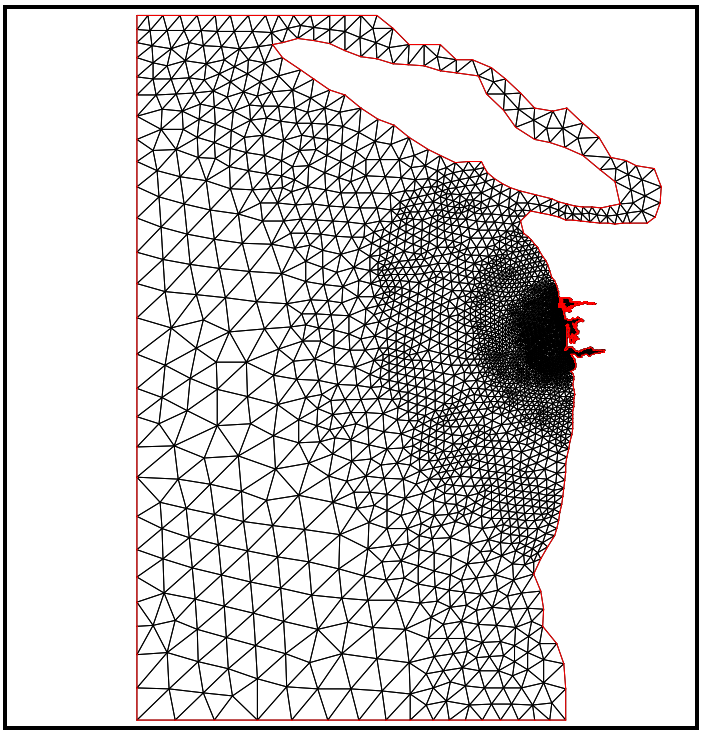

Figure 13. Domain definition and finite element grid for the Grays Harbor case

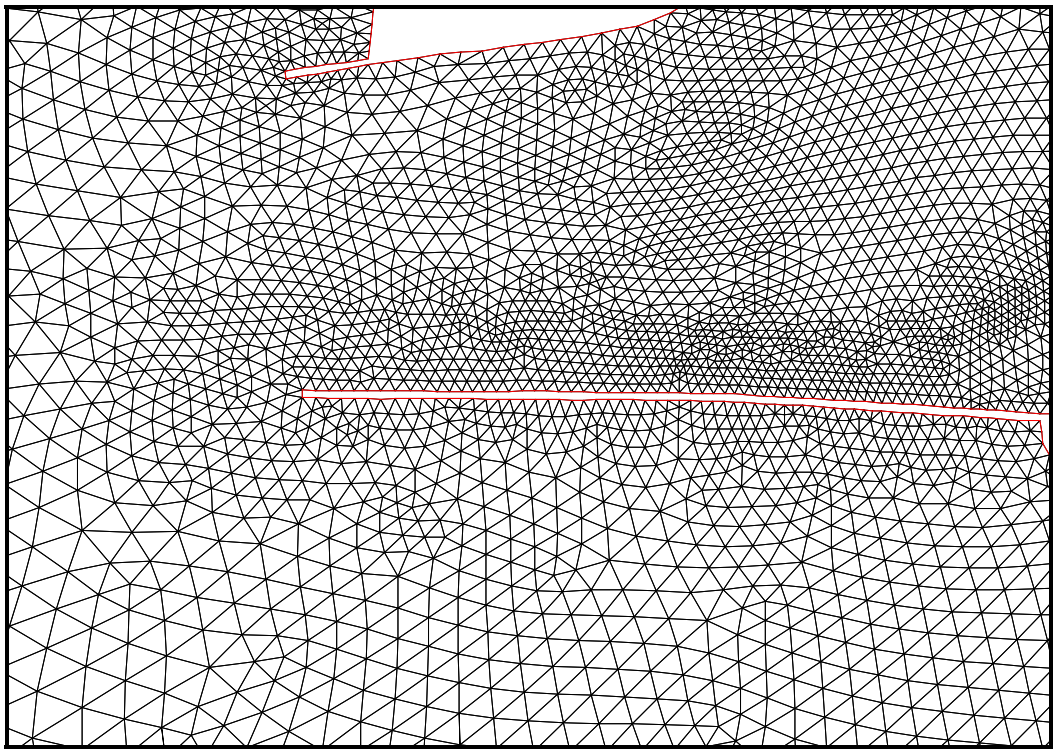

Figure 14. Detail in the area of the inlet channel

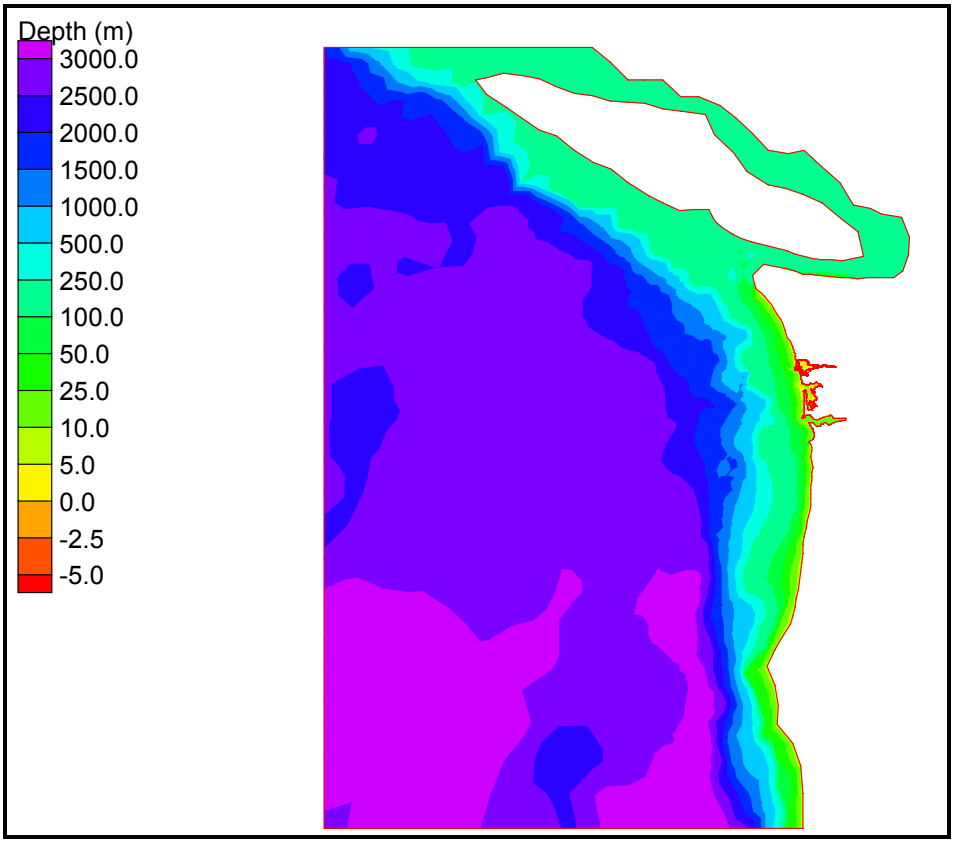

Figure 15. Definition of bathymetry in meters with respect to the geoid for Grays Harbor case

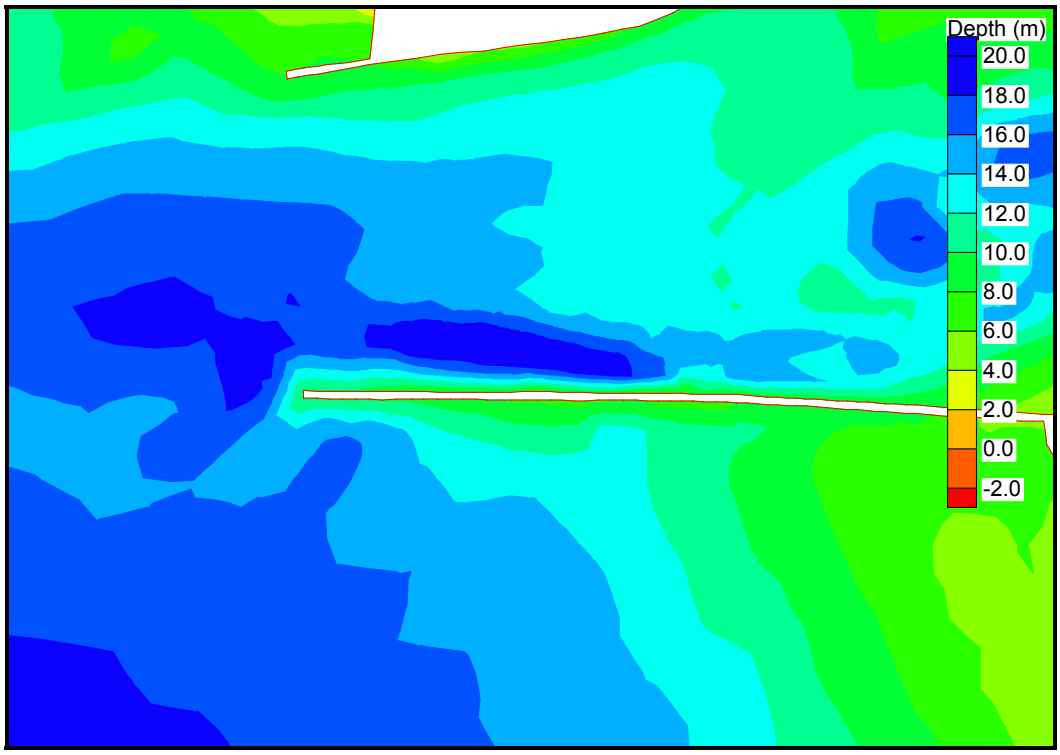

Figure 16. Detail in the area of the inlet channel

The simulation is forced with an open-ocean surface-elevation forcing and tidal potential forcing by the M_2, S_2, O_1, K_1 and N_2 constituents. Results are shown in the vicinity of the Grays Harbor inlet channel and jetty in Figures 17 through 25. Formation of an eddy along the northwestern tip of the above-water portion of the south jetty begins near slack tide at 1.64 days into the simulation (Figure 17). There is a weak south to north flow across the barrier. During the incoming tide the eddy on the north side of the jetty becomes elongated, such as at 1.66 days (Figure 18). Cross-barrier flow from south to north is present and becomes stronger. Figures 19 and 20 are snapshots at 1.70 and 1.80 days showing eastward elongation of the northern eddy with an increase in south to north cross-barrier flow. Initiation of the receding tide at 1.85 days is shown in Figure 21. The eddy north of the jetty contracts and the cross-barrier flow now reverses into a weak north to south flow. At 1.86 days into the simulation the eddy north of the south jetty becomes smaller (Figure 22). Strong ebb flows hug both the northern and southern edges of the inlet channel. Weak center channel flow and weak north-to-south flow across limited portions of the south jetty are present. Strong ebb current at 1.88 days and the formation of an eddy south of the south jetty are shown in Figure 23. The cross-barrier flow is weak. At 1.93 days the eddy to the south of the south jetty has moved away from the barrier (Figure 24). Cross-barrier flow is extremely weak at this time. At 2.05 days, the water level is near low tide (Figure 25). All eddies have disappeared and there is no cross-barrier flow.

The circulation patterns in the vicinity of Grays Harbor and its south jetty are complex. The eddies that form are small scale, the inlet velocity is fast, and the advective terms contribute significantly to the flow. If the numerical discretization and parameters are incorrectly specified, spurious spatial oscillations can be generated. Furthermore when severe spurious modes appear,

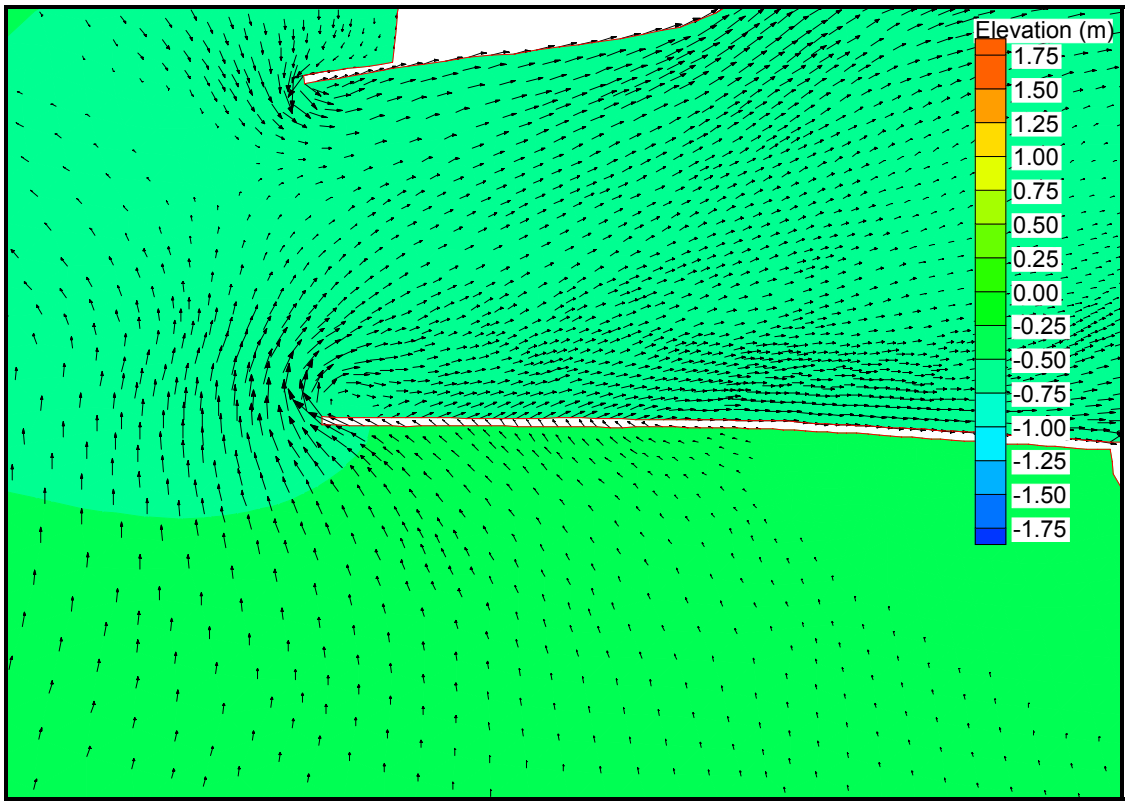

Figure 17. Grays Harbor elevation and velocity solution at time = 1.64 days

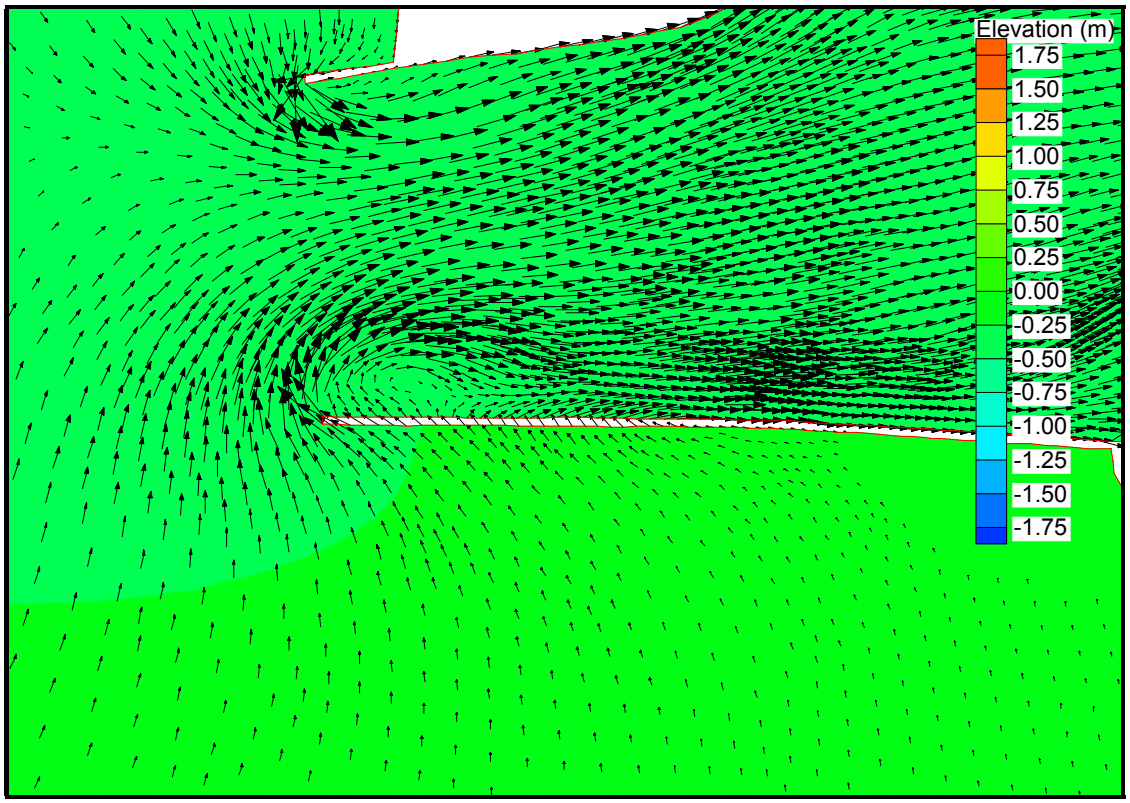

Figure 18. Grays Harbor elevation and velocity solution at time = 1.66 days

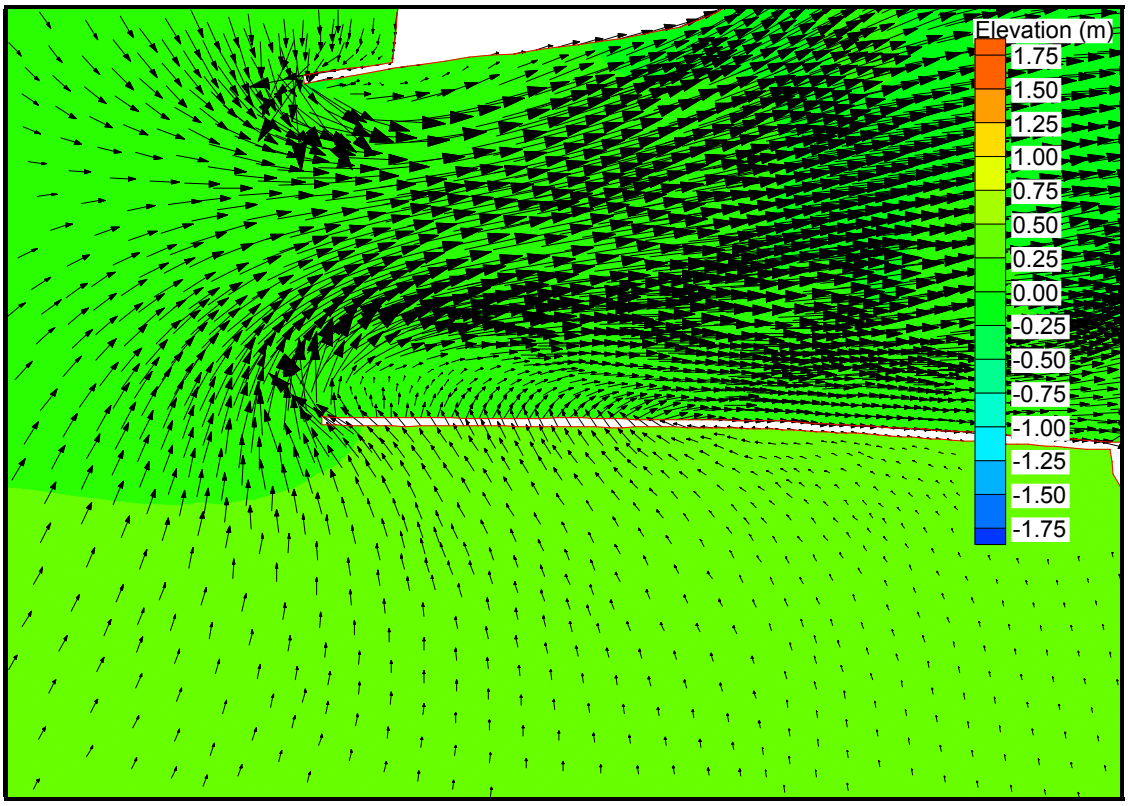

Figure 19. Grays Harbor elevation and velocity solution at time = 1.70 days

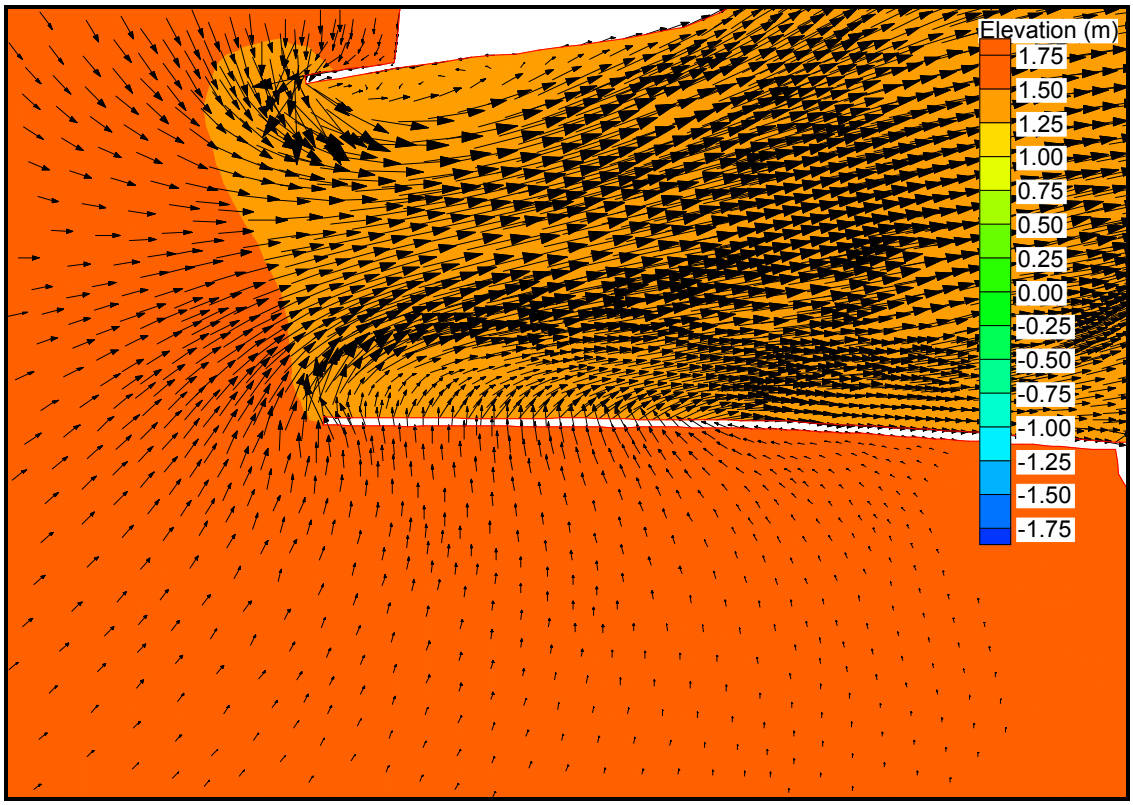

Figure 20. Grays Harbor elevation and velocity solution at time = 1.80 days

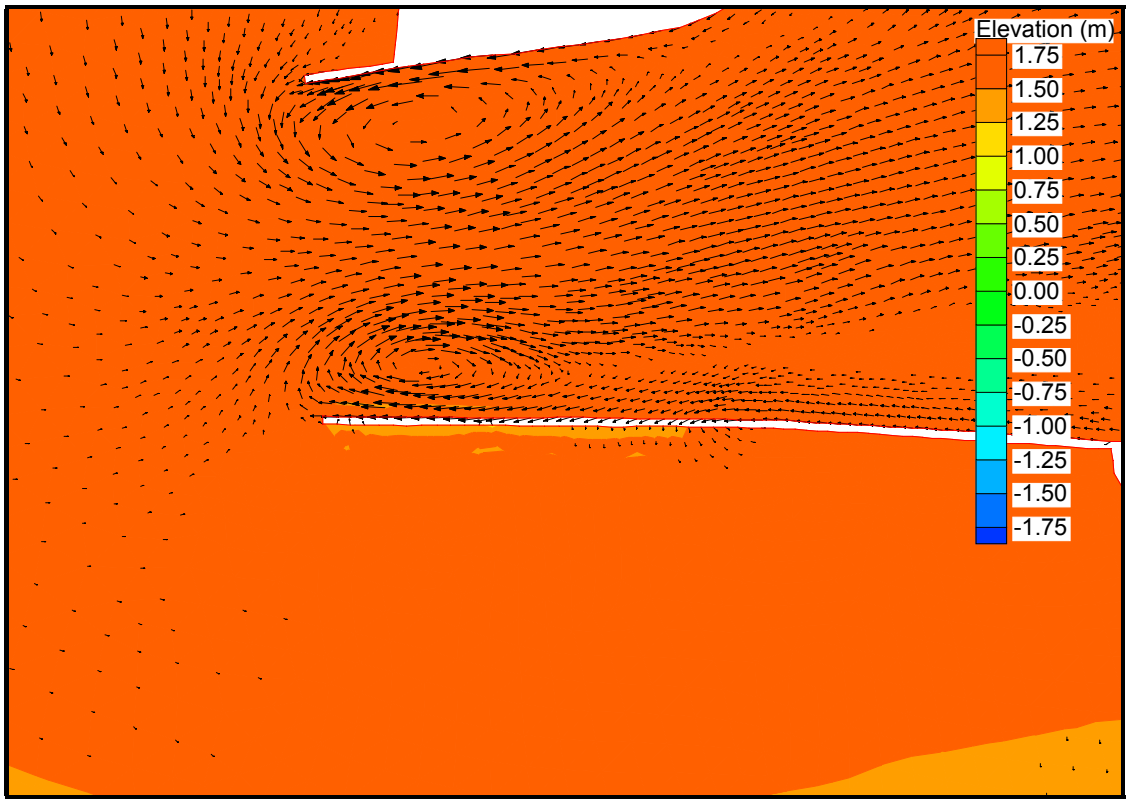

Figure 21. Grays Harbor elevation and velocity solution at time = 1.85 days

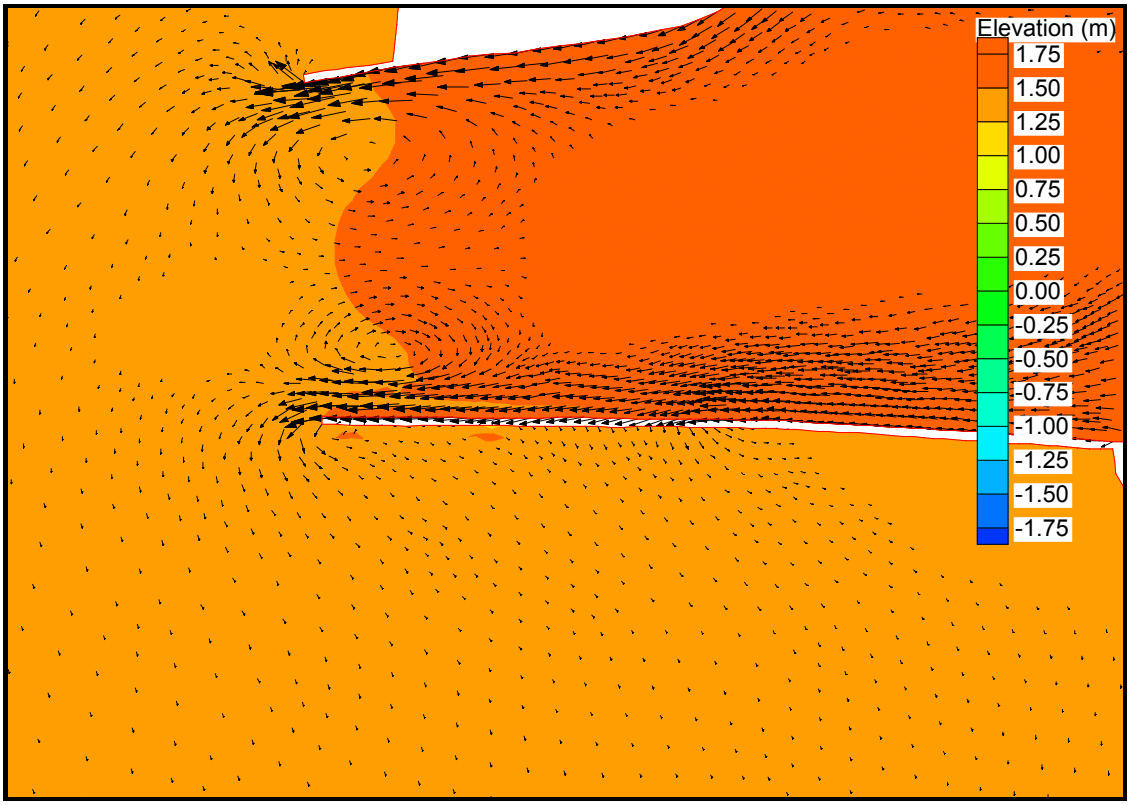

Figure 22. Grays Harbor elevation and velocity solution at time = 1.86 days

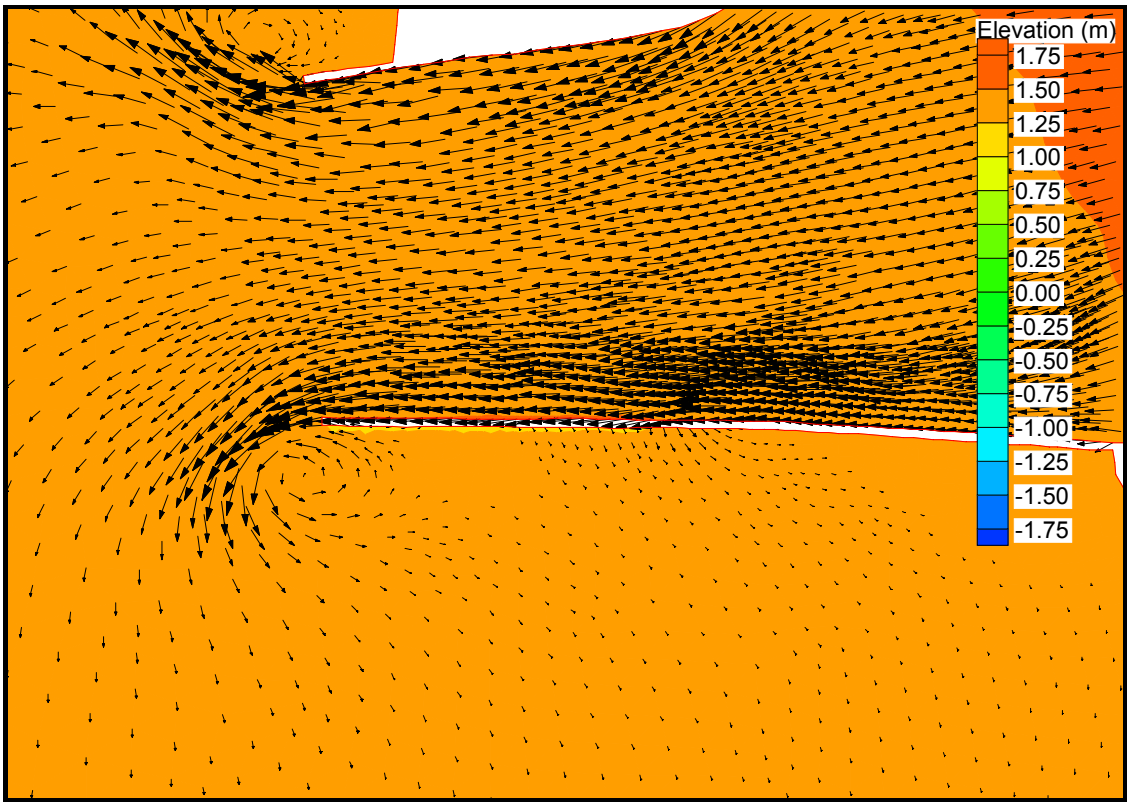

Figure 23. Grays Harbor elevation and velocity solution at time = 1.88 days

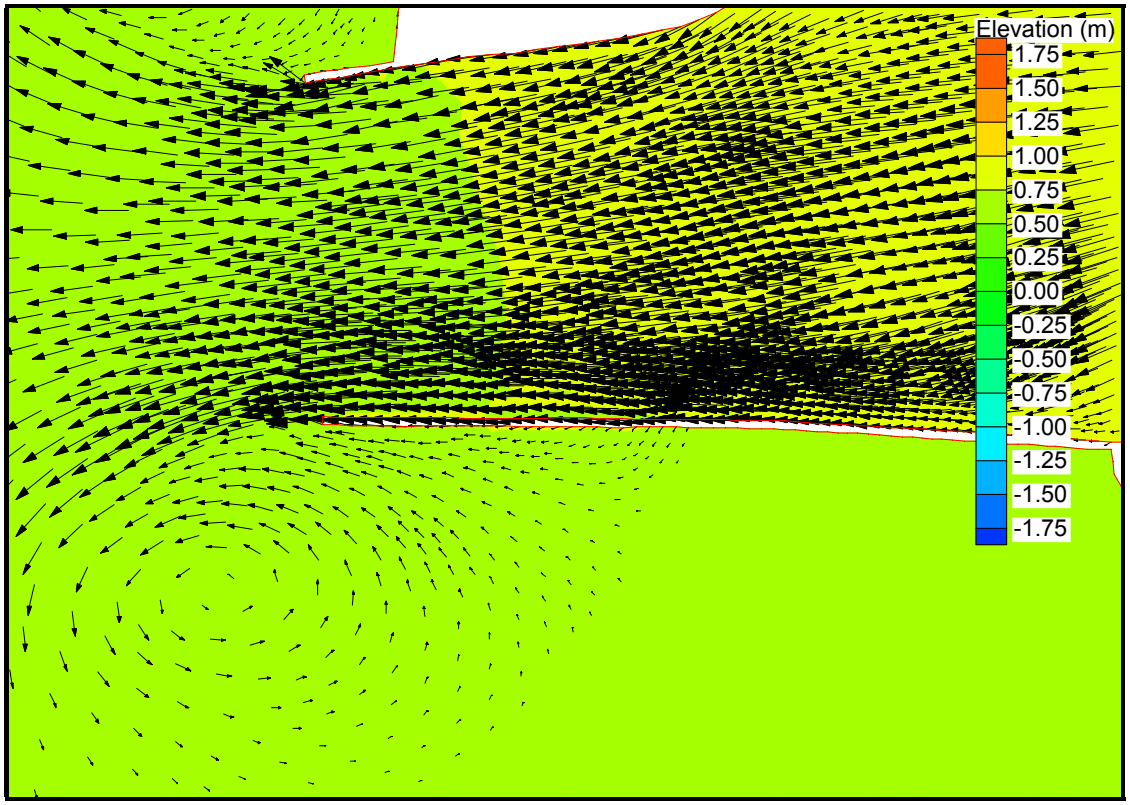

Figure 24. Grays Harbor elevation and velocity solution at time = 1.93 days

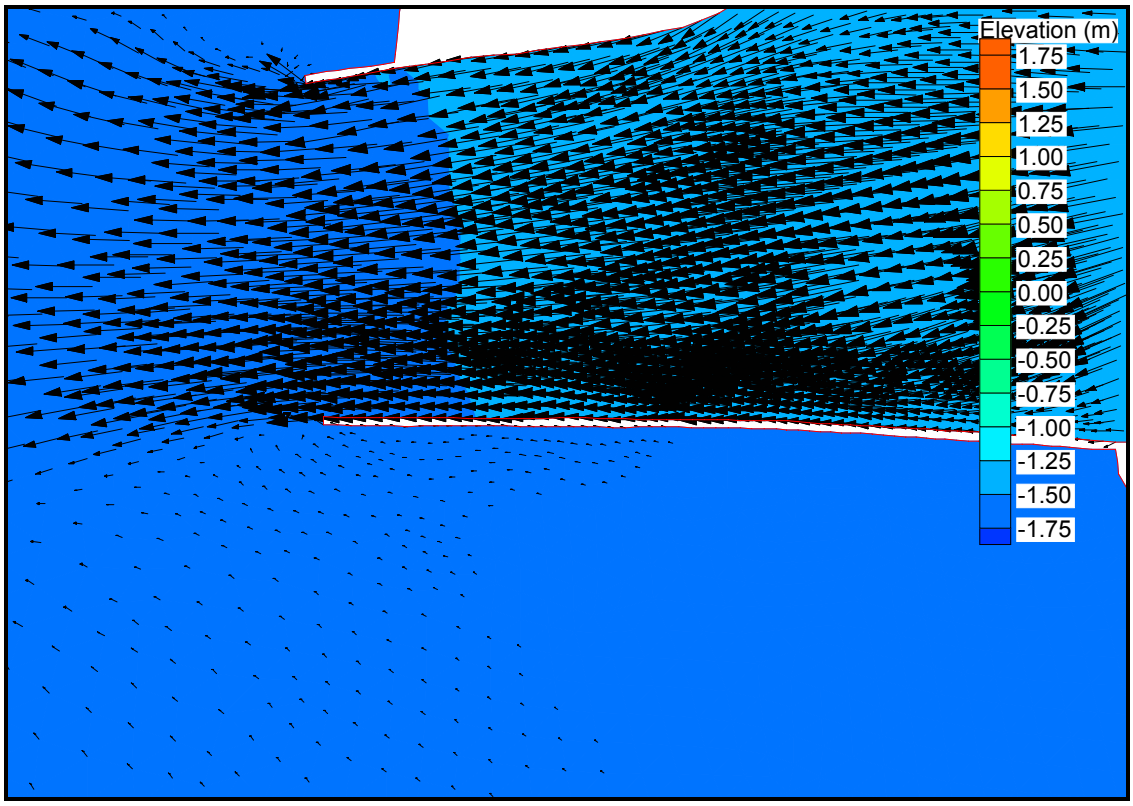

Figure 25. Grays Harbor elevation and velocity solution at time = 2.05 days

the cross-barrier boundary conditions may feed the oscillations. This situation can readily occur when the cross-barrier surface-elevation gradients are small, as they are in this example.

To avoid the generation of large localized oscillations, sufficient spatial and temporal resolution must be specified. In this case, an 80-m spatial resolution in the vicinity of the jetty is sufficient to resolve the eddies that are formed, and allow for the elimination of spurious modes associated with under-resolved grids. As a rule of thumb, at least seven nodes should be specified across any eddies that are formed. Sufficient temporal resolution is another important issue that may control the smoothness of the solution. Typically, the Courant number based on wave celerity ($C_{CW} = \sqrt{gh}\Delta t / \Delta x$ where C_{CW} = wave celerity based Courant number; g = acceleration due to gravity; h = water column depth of the flow; Δt = time-step; Δx = node to node spacing) and flow speed ($C_U = U\Delta t / \Delta x$ where C_U = flow speed based Courant number and U = flow speed) should be smaller than 0.25. Wave celerity Courant number is the limiting factor in this domain, specifically within the channel leading along the jetty into Grays Harbor. A time-step of 1 sec allows for a maximum wave celerity based Courant number equal to 0.3 in the channel region. This time-step was sufficient to eliminate spurious modes.

In addition to resolution, the GWCE-based solution requires a proper selection of the numerical parameter τ_0. Typically τ_0 should be set small in deep and intermediate tidal waters. Thus, generally but not always, waters deeper than 5 m should have a τ_0 value ranging between 0.0025 and 0.005. In very shallow tidal regions with water column depths less than 5 m and in fast flowing rivers, a value of τ_0 ranging between 0.01 and 0.02 should be specified. Note that if τ_0 is

specified too small, poor mass conservation will result and if it is set too high, spurious modes will result. Finally, it is recommended that whenever oscillations appear, the double precision version of the code be compiled and run and the iterative solver parameters CONVCR and ITMAX be set sufficiently high (for 64 bit calculations CONVCR should be at least 10^{-8} and ITMAX should be at least 25).

ADDITIONAL INFORMATION: Questions about this Technical Note can be addressed to Dr. Joannes J. Westerink (voice: 219-631-6475, e-mail: *jjw@photius.ce.nd.edu*) or Dr. Adele Militello (voice: 601-634-634-3099, e-mail: *Adele.Militello@erdc.usace.army.mil*). Information on the ADCIRC hydrodynamics model can be found at *http://www.unc.edu/depts/marine/C_CATS/adcirc/.* For information about the Coastal Inlets Research Program, please contact the Program Technical Leader, Dr. N. Kraus (voice: 601-634-2016, e-mail: *Nicholas.C.Kraus@erdc.usace.army.mil*). This Technical Note should be cited as follows:

> Westerink, J. J., Luettich, R. A., and Militello, A. (2001). "Leaky internal-barrier normal-flow boundaries in the ADCIRC coastal hydrodynamics code," Coastal and Hydraulic Engineering Technical Note CHETN IV-XX, U.S. Army Engineer Research and Development Center, Vicksburg, MS.
> *http://chl.wes.army.mil/library/publications/chetn/*

REFERENCES:

Blain, C. A., Westerink, J. J., Luettich, R. A., and Scheffner, N. W. (1993). "Generation of a storm surge data base from the hindcast of 153 historical hurricane events," Contract Report, prepared for the U.S. Army Engineer Waterways Experiment Station, Vicksburg, MS.

Blain, C. A., Westerink, J. J., and Luettich, R. A. (1994). "The influence of domain size on the response characteristics of a hurricane storm surge model," *Journal of Geophysical Research-Oceans* 99 (C9), 18467-18479.

Blain, C. A., Westerink, J. J., Luettich, R. A., and Scheffner, N. W. (1994a). "ADCIRC: An advanced three-dimensional circulation model for shelves, coasts, and estuaries; Report 4: Hurricane storm surge modeling using large domains," Headquarters, U.S. Army Corps of Engineers, Washington, DC.

Blain, C. A., Westerink, J. J., Luettich, R. A., and Scheffner, N. W. (1994b). "Generation of a storm surge time history data base from the hindcast of extratropical storm events from 1977-1992," Contract Report, prepared for the U.S. Army Engineer Waterways Experiment Station, Vicksburg, MS.

Blain, C. A., Westerink, J. J., and Luettich, R. A. (1998). "Grid convergence studies for the prediction of hurricane storm surge," *International Journal for Numerical Methods in Fluids* 26, 369-401.

Chow, V. T. (1959). *Open-channel hydraulics*. McGraw-Hill Book Co., New York.

Daugherty, R. L., Franzini, J. B., and Finnemore, E. J. (1985). *Fluid mechanics with engineering applications.* McGraw-Hill Book Co., New York.

Grenier, R. R., Luettich, R. A., and Westerink, J. J. (1994). "Comparison of 2D and 3D models for computing shallow water tides in a friction dominated tidal embayment," *Estuarine and Coastal Modeling III*, M. Spaulding et al., eds., ASCE, New York, 58-70.

Grenier, R. R., Luettich, R. A., and Westerink, J. J. (1995). "A comparison of the nonlinear frictional characteristics of two-dimensional and three-dimensional models of a shallow tidal embayment," *Journal of Geophysical Research* 100, C7, 13719-13735.

Hagen, S.C., Westerink, J.J., and Kolar, R.L. (2000). "Finite element grids based on a localized truncation error analysis," *International Journal for Numerical Methods in Fluids* 32, 241-261.

Hagen, S. C., Westerink, J. J., Kolar, R. L., and Horstmann, O. (2001). "Two dimensional unstructured mesh generation for tidal models," *International Journal for Numerical Methods in Fluids* 35, 669-686.

Hench, J. L., Luettich, R. A., Westerink, J. J., and Scheffner, N. W. (1994). "Development of a tidal constituent database for the eastern North Pacific," Headquarters, U.S. Army Corps of Engineers, Washington, DC.

Kolar, R. L., Westerink, J. J., Cantekin, M. E., and Blain, C. A. (1994a). "Aspects of nonlinear simulations using shallow water models based on the wave continuity equation," *Computers and Fluids* 23, 3, 523-538.

Kolar, R. L., Gray, W. G., Westerink, J. J., and Luettich, R. A. (1994b). "Shallow water modeling in spherical coordinates: Equation formulation, numerical implementation and application," *Journal of Hydraulic Research* 32, 1, 3-24.

Kolar, R. L., Gray, W. G., and Westerink, J. J. (1996). "Boundary conditions in shallow water models - an alternative implementation for finite element codes," *International Journal for Numerical Methods in Fluids* 22, 603-618.

Luettich, R. A., Birkhahn, R. H., and Westerink, J. J. (1991). "Application of ADCIRC-2DDI to Masonboro Inlet, North Carolina: A brief numerical modeling study," Contract Report, prepared for the U.S. Army Engineer Waterways Experiment Station, Vicksburg, MS.

Luettich, R. A., Westerink, J. J., and Scheffner, N. W. (1991). "ADCIRC: An advanced three-dimensional circulation model for shelves, coasts and estuaries; Report 1: Theory and methodology of ADCIRC-2DDI and ADCIRC-3DL," Technical Report DRP-92-6, Headquarters, U.S. Army Corps of Engineers, Washington DC.

Luettich, R. A. and Westerink, J. J. (1991). "A solution for the vertical variation of stress, rather than velocity, in a three-dimensional circulation model," *International Journal for Numerical Methods in Fluids* 12, 911-928.

Luettich, R. A., Hu, S., Westerink, J. J., and Scheffner, N. W. (1992). "Modeling 3-D circulation using the DSS technique," *Estuarine and coastal modeling.* M. Spaulding, ed., ASCE, New York.

Luettich, R. A., Hu, S., and Westerink, J. J. (1994). "Development of the direct stress solution technique for three dimensional hydrodynamic models using finite elements," *International Journal for Numerical Methods in Fluids* 19, 295-319.

Luettich, R. A. and Westerink, J. J. (1995a). "Continental shelf scale convergence studies with a baro-tropic model," *Quantitative skill assessment for coastal ocean models.* D. R. Lynch and A. M. Davies, eds., American Geophysical Union.

Luettich, R. A. and Westerink, J. J. (1995b). "An assessment of flooding and drying techniques for use in the ADCIRC hydrodynamic model: Implementation and performance in one-dimensional flows," Contract Report, prepared for Headquarters, U.S. Army Corps of Engineers, Vicksburg, MS.

Luettich, R. A. and Westerink, J. J. (1995c). "Implementation and testing of flooding and drying in the ADCIRC hydrodynamic model," Contract Report, prepared for Headquarters, U.S. Army Corps of Engineers, Vicksburg, MS.

Luettich, R. A. and Westerink, J. J. (1999). "Elemental wetting and drying in the ADCIRC hydrodynamic model: Upgrades and documentation for ADCIRC version 34.XX," Contract Report, prepared for Headquarters, U.S. Army Corps of Engineers, Vicksburg, MS.

Scheffner, N. W., Mark, D. J., Blain, C. A., Westerink, J. J., and Luettich, R. A. (1994). "ADCIRC: An advanced three-dimensional circulation model for shelves, coasts, and estuaries; Report 5: A tropical storm data base for the east and Gulf coasts of the United States," Headquarters, U.S. Army Corps of Engineers, Washington, DC.

Westerink, J. J. and Luettich, R. A. (1991). "Tide and storm surge predictions in the Gulf of Mexico using model ADCIRC-2D," Contract Report, prepared for the U.S. Army Engineer Waterways Experiment Station, Vicksburg, MS.

Westerink, J. J., Muccino, J. C., and Luettich, R. A. (1992). "Tide and storm surge computations for the Western North Atlantic and Gulf of Mexico," *Estuarine and coastal modeling.* M. Spaulding, ed., ASCE, New York.

Westerink, J. J., Luettich, R. A., Baptista, A. M., Scheffner, N. W., and Farrar, P. (1992a). "Tide and storm surge predictions using a finite element model," *Journal of Hydraulic Engineering* 118, 1373-1390.

Westerink, J. J., Luettich, R. A., Blain, C. A., and Scheffner, N. W. (1992b). "ADCIRC: An advanced three-dimensional circulation model for shelves, coasts and estuaries; Report 2: Users manual for ADCIRC-2DDI," Technical Report DRP-92-6, Headquarters, U.S. Army Corps of Engineers, Washington DC.

Westerink, J. J. (1993). "Tidal Prediction in the Gulf of Mexico/Galveston Bay using model ADCIRC-2DDI," Contract Report, prepared for the U.S. Army Engineer Waterways Experiment Station, Vicksburg, MS.

Westerink, J. J., Luettich, R. A., and Scheffner, N. W. (1993). "ADCIRC: An advanced three-dimensional circulation model for shelves, coasts and estuaries; Report 3: Development of a tidal constituent data base for the Western North Atlantic and Gulf of Mexico," Technical Report DRP-92-6, Headquarters, U.S. Army Corps of Engineers, Washington, DC.

Westerink, J. J., Luettich, R. A., and Muccino, J. C. (1994). "Modeling tides in the western North Atlantic using unstructured graded grids," *Tellus* 46A, 178-199.

Westerink, J. J., Luettich, R. A., Wu, J. K., and Kolar, R. L. (1994). "The influence of normal flow boundary conditions on spurious modes in Finite Element solutions to the shallow water equations," *International Journal for Numerical Methods in Fluids* 18, 1021-1060.

Westerink, J. J. and Luettich, R. A. (1996). "ADCIRC - version 30.02: Methodologies and input/output requirements for enhanced provisions for specified non-zero normal flow boundaries, external barrier normal flow boundaries and internal barrier normal flow boundaries," Contract Report, prepared for the U.S. Army Engineer Waterways Experiment Station, Vicksburg, MS.

Westerink, J. J. and Luettich, R. A. (1997). "Tidal predictions for Galveston Bay, Texas using model ADCIRC-2DDI," Report to the Texas Water Development Board, State of Texas, Austin TX.